

lagenase/dispase (2 mg/ml) and deoxyribonuclease (DNase) (0.1 mg/ml) for 12 to 20 min before removal of the vitreous humor, then incubated in Calcium Green-1 AM (33.3 mg/ml; Molecular Probes) and pluronic acid (4.7 mg/ml) for 1 hour at room temperature, mounted onto nitrocellulose filters, and secured in a chamber perfused at ~3 ml/min with HCO₃⁻-buffered Ringer's (24°C) [117 mM NaCl, 3 mM KCl, 2 mM CaCl₂, 1 mM MgSO₄, 0.5 mM NaH₂PO₄, 15 mM dextrose, 26 mM NaHCO₃, equilibrated with 5% CO₂ in O₂ (pH ~7.4)]. In most experiments, 2 μM ATP and 10 or 100 μM glutamate were added to the perfusate to potentiate the Ca²⁺ waves. Ca²⁺ responses were also seen without ATP and glutamate added. Glutamate concentration at the surface of the retina in vivo ranges between 10 and 400 μM [A. A. Heinamaki, A. S. H. Muhonen, R. S. Piha, *Neurochem. Res.* **11**, 535 (1986); G. Gunnarson, A.-K. Jakobsson, A. Hamberger, J. Sjöstrand, *Exp. Eye Res.* **44**, 235 (1987)].

14. Labeled glial cells were imaged with a Noran Odyssey confocal scanner and a BX60 Olympus microscope with 20× [0.5 numerical aperture (NA)] and 40× (0.8 NA) water immersion objectives. Calcium Green-1 fluorescence was monitored with 488-nm argon excitation and a 515-nm-long pass barrier filter. Images, averages of 16 video frames, were acquired every 0.93 s with MetaMorph software (Universal Imaging). Measurements were corrected for baseline drift resulting from bleaching.
15. W. T. Kim, M. G. Rioult, A. H. Cornell-Bell, *Glia* **11**, 173 (1994).
16. O. Thastrup, P. J. Cullen, B. K. Drobak, M. R. Hanley, A. P. Dawson, *Proc. Natl. Acad. Sci. U.S.A.* **87**, 2466 (1990).
17. T. K. Ghosh, P. S. Eis, J. M. Mullaney, C. L. Ebert, D. L. Gill, *J. Biol. Chem.* **263**, 11075 (1988).
18. The patch pipette solution contained 5 mM NaCl, 120 mM KCl, 1 mM CaCl₂, 7 mM MgCl₂, 5 mM EGTA, 5 mM Na₂ATP, 5 mM Hepes, 2 μM Calcium

Green-1 K_g salt, and heparin (100 μg/ml) (6 kD), and the solution was adjusted to pH 7.2 with KOH. Cells were judged to be successfully dialyzed with the pipette solution if Calcium Green-1 fluorescence in the cells increased at least 30% after achieving whole cell recording.

19. Y. Shao and K. D. McCarthy, *Cell Calcium* **17**, 187 (1995); A. C. Charles, E. R. Dirksen, J. E. Merrill, M. J. Sanderson, *Glia* **7**, 134 (1993).
20. S. R. Robinson, E. C. G. M. Hampson, M. N. Munro, D. I. Vaney, *Science* **262**, 1072 (1993).
21. V. Parpura, F. Liu, K. V. Jęftinija, P. G. Haydon, S. D. Jęftinija, *J. Neurosci.* **15**, 5831 (1995).
22. We thank P. Ceelen for technical assistance, M. H. Newman for suggestions concerning data analysis, and J. I. Gepner for helpful comments on the manuscript. Supported by NIH grants EY04077 and EY10383.

12 July 1996; accepted 29 October 1996

Joining the Two Domains of a Group I Ribozyme to Form the Catalytic Core

Michael A. Tanner and Thomas R. Cech*

Self-splicing group I introns, like other large catalytic RNAs, contain structural domains. Although the crystal structure of one of these domains has been determined by x-ray analysis, its connection to the other major domain that contains the guanosine-binding site has not been known. Site-directed mutagenesis and kinetic analysis of RNA splicing were used to identify a base triple in the conserved core of both a cyanobacterial (*Anabaena*) and a eukaryotic (*Tetrahymena*) group I intron. This long-range interaction connects a sequence adjacent to the guanosine-binding site with the domain implicated in coordinating the 5' splice site helix, and it thereby contributes to formation of the active site. The resulting five-strand junction, in which a short helix forms base triples with three separate strands in the *Tetrahymena* intron, reveals exceptionally dense packing of RNA.

Catalytic RNAs are convenient for investigating how RNA-RNA interactions determine the global folding of the molecule; their structure can be revealed by their activity. In group I introns, RNA forms the active site and directs the cleavage and ligation reactions at the 5' and 3' splice sites (1). The catalytic core of group I introns consists of two structural domains, P4-P6 and P3-P9 (2, 3). A portion of P4-P6 has been proposed to interact with the substrate helix P1 (2, 4), which contains the 5' splice site, and P3-P9 contains the binding site for the guanosine nucleophile (5). When provided as separate molecules, the P4-P6 and P3-P9 domains of the *Tetrahymena* group I intron can self-assemble into an active structure (6). These domains associate with nanomolar apparent dissociation constants, suggesting that they interact through multiple tertiary contacts.

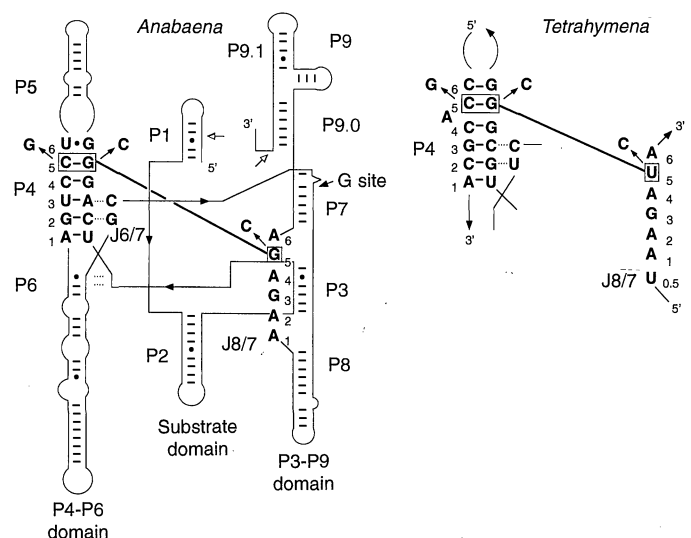
Comparative sequence analysis has been valuable for identifying potential long-range interactions in group I introns (2, 7).

Within the transfer RNA (tRNA) subgroup of group I introns, there is a weak triple correlation between the fifth base pair of P4 and the fifth base of J8/7 (8) (Fig. 1). All but one have an A·C or G·C base pair at this position in P4, and a G or U nucleotide at J8/7-5. The lone exception, *Azoarcus*, has a C·G base pair and a C at J8/7-5 (9,

10). Although this single example of covariation in the tRNA subgroup is tantalizing, it does not provide substantial evidence for the interaction. Thus, a biochemical approach was undertaken.

The well-characterized tRNA intron from the cyanobacterium *Anabaena* PCC7120 (11, 12) was used to test the importance of base pair 5 in P4 and J8/7 base 5 by site-directed mutagenesis (Fig. 1) (13). Orientation of the G·C base pair in P4 was found to be critical because a base pair flip resulted in a rate of splicing that was 2500 times lower (compare Fig. 2, A and B). The J8/7-5 G to U change (found in many tRNA introns) had wild-type activity (14), but a G to C change resulted in a 2200 times lower splicing activity (Fig. 2C). When the double mutant of P4 base pair 5 (G·C to C·G) and J8/7-5 (G to C) was tested for splicing, activity was restored; it was only eight times lower than that of wild type, a 300-fold rescue (Fig. 2D). The biphasic kinetics of reaction of the double mutant indicated that it has a residual folding problem (Fig. 3). Restoration of most of the activity with the double mutation sug-

Fig. 1. The secondary structure of the *Anabaena* tRNA^{Leu} intron with the proposed tertiary interaction highlighted. Domain organization (27) is shown with splice sites marked by open arrows; the mutations are shown next to the wild-type sequence. P stands for paired region; J stands for joining region; for example, J8/7 joins P8 and P7. (Right) The relevant portions of the *Tetrahymena* ribosomal RNA intron; in this case, P4 contains a bulged A residue not conserved among group I introns.



Department of Chemistry and Biochemistry, Howard Hughes Medical Institute, University of Colorado, Boulder, Colorado 80309-0215, USA.

*To whom correspondence should be addressed.

gests an interaction between base J8/7-5 and base pair 5 in P4 in the *Anabaena* intron (Fig. 1).

In the case of the *Tetrahymena* intron, changing the identity of the equivalent bases in P4 and J8/7 (15) had little effect on

splicing activity *in vivo*, when an *Escherichia coli* β -galactosidase gene interrupted by the intron was used (16), or *in vitro* under the standard splicing conditions (30°C) (Table 1). However, intron circularization, a post-splicing reaction (17), was reduced in

both the P4 base pair 5 and J8/7-5 single mutants, whereas the double mutation of P4 base pair 5 and J8/7-5 restored intron circularization (14). This observation suggested that these distant sites in the secondary structure might be interacting in the active molecule.

We tested splicing under more destabilizing conditions of higher temperatures; because the domains of the *Tetrahymena* intron are probably assembled through multiple interactions (18), eliminating a single interaction may be insufficient to impair splicing at low temperature. At 50°C the P4 base pair 5 and J8/7-5 mutants showed an approximately five times reduced activity, unlike the situation at 30°C (Table 1). More important, the double mutant had activity restored to 68% of that of the wild type. When the *Tetrahymena* intron was reacted at 61°C, the P4 base pair 5 and J8/7-5 mutants showed even greater reduction in activity relative to the wild type, whereas the double mutation restored activity to near that of the wild-type (Table 1).

The specificity of interactions with the J8/7-5 base was tested in *Tetrahymena* by mutation of base pairs adjacent to base pair 5 in P4 and measurement of splicing at 50°C. In the context of the J8/7-5 mutation, inverting base pair 4 (G-C to C-G) gave 1.7-fold recovery of activity relative to J8/7-5 alone (restoration to 41% of the wild-type activity) (14). This was not as much as the 2.8 times recovery provided by inverting base pair 5 [restoration to 68% of that of the wild type (Table 1)]. Two possible reasons for the partial compensation at the neighboring base pair are (i) the base pair 5 change may provide a more favorable context for some residual interaction of base pair 4 with the mutant J8/7 base (20), or (ii) there may be enough flexibility in the active site such that the J8/7 base can interact productive-

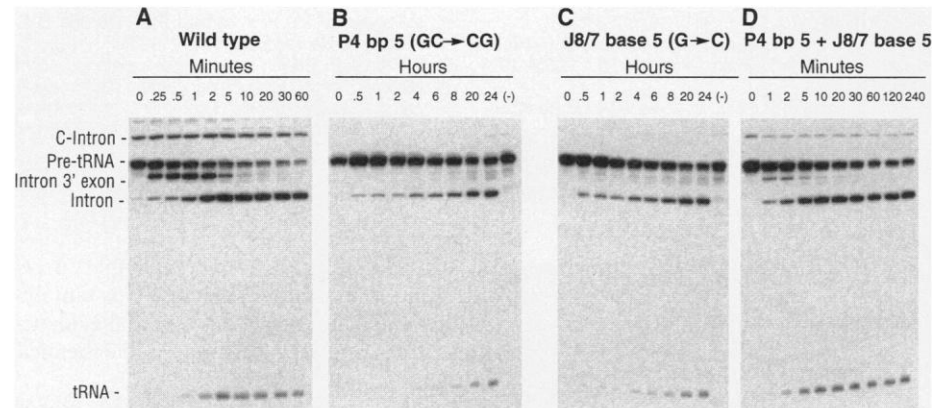


Fig. 2. Compensatory mutations rescue splicing of the *Anabaena* pre-tRNA^{Leu}. Precursor was first incubated at 50°C in 15 mM MgCl₂ and 25 mM Hepes, pH 7.5, for 5 min to initiate folding. After being cooled to 32°C, reactions were started by the addition of guanosine to 25 μ M. Splicing reactions were stopped by addition of an equal volume of stop buffer containing 30 mM EDTA and products were separated on an 8% polyacrylamide-8 M urea gel. (A) Reaction of the wild-type intron. During the first step of splicing, the guanosine becomes covalently attached to the 5' end of the intron forming the intron-3' exon intermediate and the 5' exon (run off the gel). The second step of splicing produces the linear intron and the ligated exons (tRNA). A circular intron (C-Intron) appears during the 50°C preliminary incubation (12). (B) P4 base pair 5 mutant with G-C changed to C-G. The (-) lane shows precursor reacted in the absence of guanosine for 24 hours. (C) J8/7-5 G changed to C. (D) The double mutant of P4 base pair 5 and J8/7-5.

Fig. 3. Quantitation of splicing of the *Anabaena* pre-tRNA. Splicing conditions were as in Fig. 2. (■) Wild-type intron, $k_{obs} = 1.1 \pm 0.16 \text{ min}^{-1}$. (●) The double mutant P4 base pair 5 + J8/7-5, $k_{obs} = 0.14 \pm 0.064 \text{ min}^{-1}$. (◆) The single mutant of P4 base pair 5, $k_{obs} = 4.4 (\pm 1.2) \times 10^{-4} \text{ min}^{-1}$. (▲) The single mutant of J8/7-5, $k_{obs} = 5.0 (\pm 1.7) \times 10^{-4} \text{ min}^{-1}$. Rate constants were derived from the initial linear phase of the reaction, \pm SD of three independent determinations. Reactions quantitated with a PhosphorImager (Molecular Dynamics).

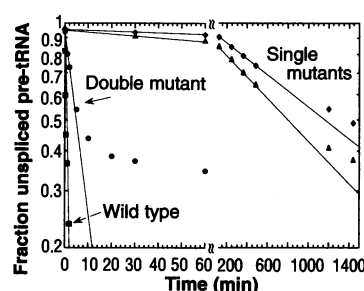
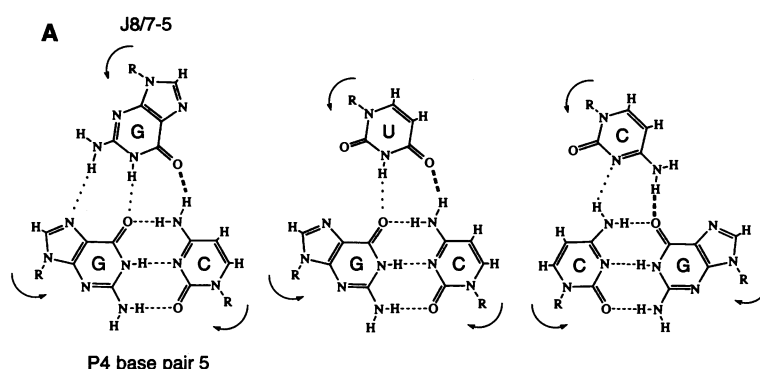


Fig. 4. (A) Proposed hydrogen bonding scheme for the base triples between P4 base pair 5 and J8/7-5. Arrows denote strand polarity. (Left) The wild-type combination in the *Anabaena* intron. (Middle) The wild-type combination in the *Tetrahymena* intron; introduction of this mutation in the *Anabaena* intron did not impair splicing. (Right) The compensatory multiple mutation that restored splicing activity in both mutant introns. The H-bonding scheme shown requires nonlinear H bonds. Alternatively, pairing could be accomplished with only the dashed or only the dotted H bonds, in which case linearity can be achieved by translation and rotation of the top bases from the positions shown. (B) P4 coordinates three single strands to form a five-



strand junction in the *Tetrahymena* intron core. Dotted lines represent base triples: 1, interdomain triple in major groove (this study); 2, triple helical scaffold in major groove (24); 3, A-rich bulge of P5abc extension provides minor groove triples (27). Boxed A's in J4/5, proximity to reaction site helix P1 (4). Circled A in J4/5, proximity to G in G-site (28). G with arrow, G-site (5).

Table 1. Splicing activity of the mutant *Tetrahymena* introns relative to that of the wild type. Conditions of splicing were: 5 mM Mg²⁺, 200 mM NaCl, 30 mM Hepes, pH 7.5. The guanosine triphosphate (GTP) concentration was adjusted to keep the rate of splicing within a range that could be measured with precision. The kinetic parameters at 30°C and 50°C did not vary by more than a factor of 2 in an independent determination; those at 61°C are averages of at least three experiments, with the double mutant having activity >10-fold that of either single mutant in every experiment.

	30°C	50°C	61°C
Wild type	(1)*	(1)†	(1)‡
P4 bp 5	0.49	0.17	0.031
J8/7-5	0.73	0.24	0.014
P4 bp 5 + J8/7-5	0.73	0.68	0.31

* $k_{\text{obs}} = 0.79 \text{ min}^{-1}$ (100 μM GTP). † $k_{\text{obs}} = 1.9 \text{ min}^{-1}$ (1 μM GTP). ‡ $k_{\text{obs}} = 0.8 \text{ min}^{-1}$ (3 μM GTP).

ly with either base pair 4 or 5 of P4. When a G·C to C·G mutation at P4 base pair 6 was combined with the J8/7-5 mutation, the resulting RNA was much less active than either single mutant (14). This suggested that base pair 6 is involved in a different interaction that is also functionally important.

Recently the crystal structure of the P4-P6 domain of the *Tetrahymena* group I intron was solved (21), providing structural detail of the base pair in P4 postulated to interact with base J8/7-5. If we assume that this crystal structure accurately represents the conformation of P4 within the intact intron, the major groove of P4 appears more accessible than its minor groove because of some steric blockage by the P5c region.

When candidates for isosteric base triples in the major groove are considered, the set shown in Fig. 4A provides a good fit to the mutagenesis data. The equivalence of G and U (in J8/7) in binding to the G·C base pair is explained (Fig. 4A, left and center) as is the requirement for a U to C transition upon flipping the G·C pair (Fig. 4A, right). In contrast, the nonfunctional combinations (G·C)C, (C·G)G and (C·G)U are ones that would lead to amine-amine repulsion or repulsion between lone pairs of electrons on two carbonyl oxygens. Evidence for such an H-bonding scheme is found in DNA triples proposed as intermediates in

homologous recombination (22) and in DNA crystal structures showing (G·C)G base triples (23). Although direct hydrogen bonding of the three bases provides an explanation for our data, we cannot exclude indirect interactions mediated by water molecules, metal ions, or other nucleotides.

Evidence for the triple base combinations shown with the dashed lines in Fig. 4A was provided by Michel *et al.* (24) and Green and Szostak (25) for the portion of the "triple helical scaffold" in the *SunY* and *Tetrahymena* introns that involves base pairs 2 and 3 of P4 pairing with J6/7 (Fig. 1). This triple helix in the major groove of the bottom half of P4 could provide stacking interactions to stabilize the base triple with J8/7, essentially continuing the triple helix. We therefore propose that P4 is a structural organization center for the entire core (Fig. 4B), simultaneously interacting with J6/7 and J8/7 in its major groove and (in the *Tetrahymena* subclass of group I introns) binding the P5a A-rich bulge in its minor groove (21).

We have provided experimental support for a long-range base triple that bridges the two domains in the core of two different group I introns. Group II introns, ribonuclease P RNA, and ribosomal RNA are also composed of domains of tertiary structure, and interdomainal interactions are being identified (26). Whether base triples, originally found in the structural core of tRNA, provide a common solution to the problem of packing domains together to assemble RNA active sites remains to be seen.

REFERENCES AND NOTES

1. T. R. Cech, *Annu. Rev. Biochem.* **59**, 543 (1990).
2. F. Michel and E. Westhof, *J. Mol. Biol.* **216**, 585 (1990).
3. F. L. Murphy and T. R. Cech, *Biochemistry* **32**, 5291 (1993); *J. Mol. Biol.* **236**, 49 (1994).
4. J.-F. Wang, W. D. Downs, T. R. Cech, *Science* **260**, 504 (1993).
5. F. Michel *et al.*, *Nature* **342**, 391 (1989).
6. J. A. Doudna and T. R. Cech, *RNA* **1**, 36 (1995).
7. D. Gautheret, S. H. Damberger, R. R. Gutell, *J. Mol. Biol.* **248**, 27 (1995).
8. R. R. Gutell, unpublished data.
9. B. Reinhold-Hurek and D. A. Shub, *Nature* **357**, 173 (1992).
10. M. A. Tanner and T. R. Cech, *RNA* **2**, 74 (1996).
11. M.-Q. Xu *et al.*, *Science* **250**, 1566 (1990); A. J. Zaug, J. A. Dávila-Aponte, T. R. Cech, *Biochemistry* **33**, 14935 (1994); B. L. Golden and T. R. Cech, *ibid.* **35**, 3754 (1996).
12. A. J. Zaug, M. M. McEvoy, T. R. Cech, *Biochemistry* **32**, 7946 (1993).
13. Polymerase chain reaction (PCR) was used to construct the mutants as follows: Clone pAtRNA-1 encoding the *Anabaena* pre-tRNA (12) was used as the template for PCR. Oligodeoxynucleotides containing the appropriate change (or changes) were used as primers to generate the full-length pre-tRNA plus a T7 promoter. Sequences were confirmed by dideoxynucleotide sequencing. PCR amplified DNA was transcribed with T7 RNA polymerase in the presence of [α -³²P]ATP, and the RNA was gel-purified as described (10).
14. M. A. Tanner and T. R. Cech, unpublished data.
15. The *Tetrahymena* intron mutants were constructed by PCR as before and cloned into the pBGST7 vector (16) at the unique restriction sites Sph I (in P2) and Nhe I (in P9). Preparation of precursor RNA was the same as for *Anabaena* (13).
16. J. V. Price and T. R. Cech, *Science* **228**, 719 (1985); M. D. Been and T. R. Cech, *Cell* **47**, 207 (1986).
17. A. J. Zaug, P. J. Grabowski, T. R. Cech, *Nature* **301**, 578 (1983); K. Ehrenman *et al.*, *Proc. Natl. Acad. Sci. U.S.A.* **83**, 5875 (1986); H. F. Tabak *et al.*, *Cell* **48**, 101 (1987).
18. The *Tetrahymena* intron contains extra sequence elements in P2.1, the P5abc extension, and the P9 extension, some of which stabilize the core (3, 19). The *Anabaena* intron lacks these extra elements and presumably relies more on core interactions for folding of the active site.
19. G. F. Joyce, G. van der Horst, T. Inoue, *Nucleic Acids Res.* **17**, 7879 (1989); B. Lagerbauer, F. L. Murphy, T. R. Cech, *EMBO J.* **13**, 2669 (1994); P. P. Zarrinkar and J. R. Williamson, *Nucleic Acids Res.* **24**, 854 (1996).
20. Context effects on base triples have been observed in tRNA by comparative analysis [R. R. Gutell *et al.*, *Nucleic Acids Res.* **20**, 5785 (1992)] and experimentally in the triple helix scaffold of group I introns (24, 25).
21. J. H. Cate *et al.*, *Science* **273**, 1678 (1996).
22. S. Lacks, *Genetics* **53**, 207 (1966); V. B. Zhurkin *et al.*, *J. Mol. Biol.* **239**, 181 (1994).
23. S. C. Schultz, G. C. Shields, T. A. Steitz, *Science* **253**, 1001 (1991); L. V. Meervelt *et al.*, *Nature* **374**, 742 (1995); D. Vlieghe *et al.*, *Science* **273**, 1702 (1996).
24. F. Michel *et al.*, *Nature* **347**, 578 (1990).
25. R. Green and J. W. Szostak, *J. Mol. Biol.* **235**, 140 (1994).
26. M. E. Harris *et al.*, *EMBO J.* **13**, 3953 (1994); A. M. Pyle and J. B. Green, *Biochemistry* **33**, 2716 (1994); M. Costa and F. Michel, *EMBO J.* **14**, 1276 (1995); T. Pan, *Biochemistry* **34**, 902 (1995); for ribosomal RNA, see R. R. Gutell, in *Ribosomal RNA*, R. A. Zimmermann and A. E. Dahlberg, Eds. (CRC Press, Boca Raton, FL, 1996), pp. 111-128, and references therein.
27. T. R. Cech, S. H. Damberger, R. R. Gutell, *Nature Struct. Biol.* **1**, 273 (1994).
28. J.-F. Wang and T. R. Cech, *Science* **256**, 526 (1992).
29. Supported by NIH grant GM28039, and the Howard Hughes Medical Institute (T.C.R.). We thank the W. M. Keck Foundation for support of RNA Science on the Boulder campus; R. Gutell for assisting us with sequence analysis; R. Gutell and B. Golden for comments on the manuscript; and C. Grosshans and E. Podell for synthesizing oligodeoxynucleotides.

24 July 1996; accepted 29 October 1996